

conduit until, near the surface, the pressure drops to the triple point (1.65×10^{-2} bar). We can follow the energetics using an isentropic path in the temperature–entropy diagram for SO_2 given by Smith *et al.*⁷. At the triple point, the liquid begins to crystallise and the system expands isothermally and isobarically with the formation of SO_2 vapour. An expanding effervescent mixture will now form, with each unit volume of liquid producing 5,000 times its volume of vapour. If the vapour and crystallising liquid remain in contact, the solid–fluid mixture will continue to expand until reaching the ambient atmospheric pressure ($\sim 10^{-7}$ bar) at or just outside the vent. On reaching the ambient pressure, the SO_2 solid–vapour mixture will have a total vapour content of $\sim 20\%$ by mass and an exit velocity of a little more than 350 ms^{-1} . The maximum range that can be reached by SO_2 snow issuing from a vent at this velocity is about 70 km for trajectories inclined $\sim 45^\circ$ to the horizontal. Depending on the orientation of individual vents, however, much of the distributed SO_2 snow would be expected to fall within a few tens of kilometres of the scarps. This is completely consistent with the scale of the diffuse white features seen in *Plate 3* and we propose

Received 19 July; accepted 3 August 1979.

1. Sharp, R. P. *J. geophys. Res.* **78**, 4063–4072 (1973).
2. Carr, M. H. *J. geophys. Res.* (in the press).
3. Smith B. A. *et al. Science* **204**, 951–971 (1979).
4. Pearl, *et al. Nature* **280**, 755–758 (1979).
5. Johnson, T. V., Cook II, A. F., Sagan, C. & Soderblom, L. A. *Nature* **280**, 746–750 (1979).
6. Strom, R. G., Terriile, R. J., Masursky, H. & Hansen, C. *Nature* **280**, 733–736 (1979).
7. Smith, B. A., Shoemaker, E. M., Keiffer, S. W. & Cook, A. F. II *Nature* **280**, 738–743 (1979).
8. Kumar, S. *Nature* **280**, 758–760 (1979).
9. Fanale, F. P. *et al. Nature* **280**, 761–763 (1979).
10. Smythe *et al. Nature* **280**, 766 (1979).
11. Carr, M. H. *Nature* **280**, 729–733 (1979).
12. Lucchita, B. K. *J. Res. U.S. Geol. Surv.* **16**, 128–137 (1977).
13. Sagan, C. *Nature* **280**, 750–753 (1979).

The role of SO_2 in volcanism on Io

B. A. Smith*, E. M. Shoemaker†, S. W. Kieffer† & A. F. Cook II‡

* Department of Planetary Sciences, University of Arizona, Tucson, Arizona 85721

† US Geological Survey, Flagstaff, Arizona 86001

‡ Smithsonian Astrophysical Observatory, Cambridge, Massachusetts 02138

Io and Earth are the only planetary bodies known to be volcanically active; the energetics of the eruptive plumes on Io have important structural implications and are closely linked with the presence of sulphur and SO_2 .

VOLCANIC plumes observed on Io by Voyager 1 reach heights between 70 and 280 km^{1,2}, implying vent ejection velocities ranging from several hundreds of metres to nearly a thousand metres per second (Table 1). At least eight vents were active at the time of Voyager 1 encounter and both recent and current activity of others seems likely². Although evidence for volcanism is found on the Moon, Mars and Mercury, Io is the only planetary body other than the Earth known to have active volcanism, and the impressive rate at which volcanic material is being deposited on the surface of this highly active planet has profound implications for its bulk chemical evolution³. Here we examine the energetics of the eruptive plumes and the implications for the structure, the ground fluid ‘hydrology’ and hydrological cycle of Io’s crust.

The driving energy for Io’s intense volcanism seems likely to be the model proposed by Peale *et al.*⁴ where tidal energy is dissipated in a thin crust surrounding a completely molten interior. In this model, runaway melting takes place within a small molten core and is stabilised only when the solid mantle or crust becomes sufficiently thin to conduct away all of the tidally generated heat. Because this mechanism is sustained by the forced eccentricity of Io’s orbit which arises chiefly from perturbation by Europa, it probably existed throughout much of geologic time and should continue almost indefinitely. If we assume that the current resurfacing rates³ are applicable over geological time scales, Io’s crust must have been recycled many times over while in contact, at its base, with a convective interior. Thus, early loss and eventual depletion of volatiles from the bulk composition of Io would be expected. In explaining current

that artesian SO_2 volatilisation, solidification and ballistic deposition is the source of these features.

The most likely initial escape route would be along a fresh boundary fault. This type of scarp, which is usually relatively straight and smooth surfaced, would rapidly become scalloped, notched and irregular in appearance, due to the energetic venting of SO_2 gas and snow along its face. This sapping process would work together with slumping and other mass wasting processes to create the erosional patterns observed. The release of the aquifer would continue until local equilibrium was attained. Recharge of SO_2 in the aquifer should cause further venting and continued erosion of the scarps. This process of venting and sapping would continue until the SO_2 is locally depleted (for example, the inselbergs) in which case further cliff retreat could occur only by mass wasting working alone. We thus propose that the fretted terrains on Io and those on Mars are formed by analogous sapping mechanisms in which liquid SO_2 provides the analogue to H_2O in terrestrial (and martian) aquifers.

volcanism on Io, we must consider those materials with vapour pressures sufficiently low to have survived aeons of crustal and internal recycling.

Fundamental to our analysis is the probable presence of SO_2 frost or adsorbed SO_2 on the surface of Io^{5,6} and the recognition that SO_2 is a prominent constituent of its atmosphere^{3,7–9}. Noting also the discovery of ionised S and O in the Io torus^{10,11}, the spectrophotometric suggestion of elemental sulphur on its surface^{12–15}, and the absence of both H_2O bands and the broad absorption features associated with iron-bearing silicates, we conclude that SO_2 is the volatile which drives pyroclastic volcanism on Io and that sulphur and SO_2 are the primary constituents of the uppermost crust and subjacent molten zone. Other constituents are certainly present (Na and K are observed to be escaping from Io), but probably occur in minor quantities.

The mechanism that drives violent gaseous eruptions in terrestrial volcanoes is the rapid expansion of volatiles, primarily H_2O and CO_2 , which may either be dissolved in the silicate magma or raised to high temperature ($\sim 1,500 \text{ K}$) by contact with magma intrusions. Although vent velocities of hundreds of metres per second have been observed in terrestrial volcanic eruptions¹⁶, interaction with the terrestrial atmosphere limits the heights of volcanic plumes to a few tens of kilometres at the most. This is not the case on Io, where venting gases abruptly enter a near-vacuum environment.

Limiting velocities of a fluid or fluidised system expelled from a volcanic vent can be estimated using a simple model of adiabatic decompression of the system as it moves upwards through a passageway connecting a chamber or arbitrary depth with the surface. Assuming reversible adiabatic flow and chemical equilibrium, mass flow up the volcanic conduit can be considered to be isentropic. For such a simplified process, the thermodynamic path of the erupting material during ascent is easily envisioned on a temperature–entropy phase diagram, shown in Fig. 1 for SO_2 .

Table 1 Heights of volcanic plumes on Io

Io volcanic plumes (no.)	Maximum height above the surface* (km)	Vent velocity (ms ⁻¹)
1	280	930
2	100	580
2	210	810
(UV component)		
3	70	490
4	95	570
5	80	520
6	80	520
7	120	630
8	70	490

* After Strom *et al.*².

Several qualitatively different eruption styles are possible, depending on the entropy of the system at the time the eruption begins. High velocities of the system are attained after a vapour phase is formed. This can occur when a fluid system rising from depth is decompressed below the critical point, for cases of high entropy, or when the boundary of the liquid+vapour field is reached, for cases of low entropy. It can also occur if the system remains in place until its temperature is raised (by intrusion of a hot mass) to the point where boiling begins.

If a system such as SO₂ has an entropy less than the critical point entropy when vapourisation begins, and if the vapour and liquid phases do not separate, then, on isentropic expansion during ascent of the system to the surface, vapour will continuously evolve as the system varies along an isentrope passing through the liquid+vapour field (see line ABC in Fig. 1) until the triple point (0.0165 bar for SO₂) is intercepted. At this point, remaining liquid in the system crystallises to a lower entropy solid, and vapour is added simultaneously, causing the system to expand isobarically and isothermally until all the liquid phase disappears. Further decompression along the same isentrope results in condensation of SO₂ ice from the vapour phase; complete expansion to 0 K would result in condensation of all the vapour.

Assuming complete thermodynamic equilibrium and steady-state flow, the specific kinetic energy available for fluid motion at any pressure or temperature on ascent of the system to the surface is the difference between the initial specific enthalpy, H_0 , and the enthalpy of the products, H minus the specific potential energy gained by rise in a gravity field. For one dimensional flow,

$$\frac{u^2}{2} = H_0 - H - \int g \, dh \tag{1}$$

where u is the velocity of the system; g the gravitational acceleration; and h the height of the system.

The enthalpy of the products is

$$H = xH_v + (1-x)H_{l,ors} \tag{2}$$

where H_v and $H_{l,ors}$ are the enthalpies of the vapour, liquid or solid phases, and x is the mass fraction of vapour present; x is obtainable from the isobaric chord ratios in Fig. 1 or, numerically, from

$$x = \frac{S - S_{l,ors}}{S_v - S_{l,ors}} \tag{3}$$

where S , S_v , $S_{l,ors}$ are the total entropy, and vapour, liquid, or solid entropies respectively.

As a specific example of flow at an entropy less than the critical point entropy, consider flow from a liquid SO₂ reservoir at 40 bar and 393 K (representing flow initiating from contact with pure sulphur on its liquidus temperature of 393 K at approximately 1.5 km depth). The entropy of the SO₂ system is 2.90 J g⁻¹ K⁻¹ (point A in Fig. 1) and its initial specific enthalpy is 530 J g⁻¹. Formation of vapour in the SO₂ system initiates upward movement of the two-phase (liquid+vapour) system and the material flows up the volcanic vent with continuous evolution of vapour and increasing velocity until the triple point is reached. At this point, the SO₂ constitutes a liquid-vapour fluidised system consisting of 45% (mass fraction) vapour and, neglecting small values of $\int g \, dh$, is moving at 430 m s⁻¹ (Table 2). If it is assumed that the vent discharges at pressures in

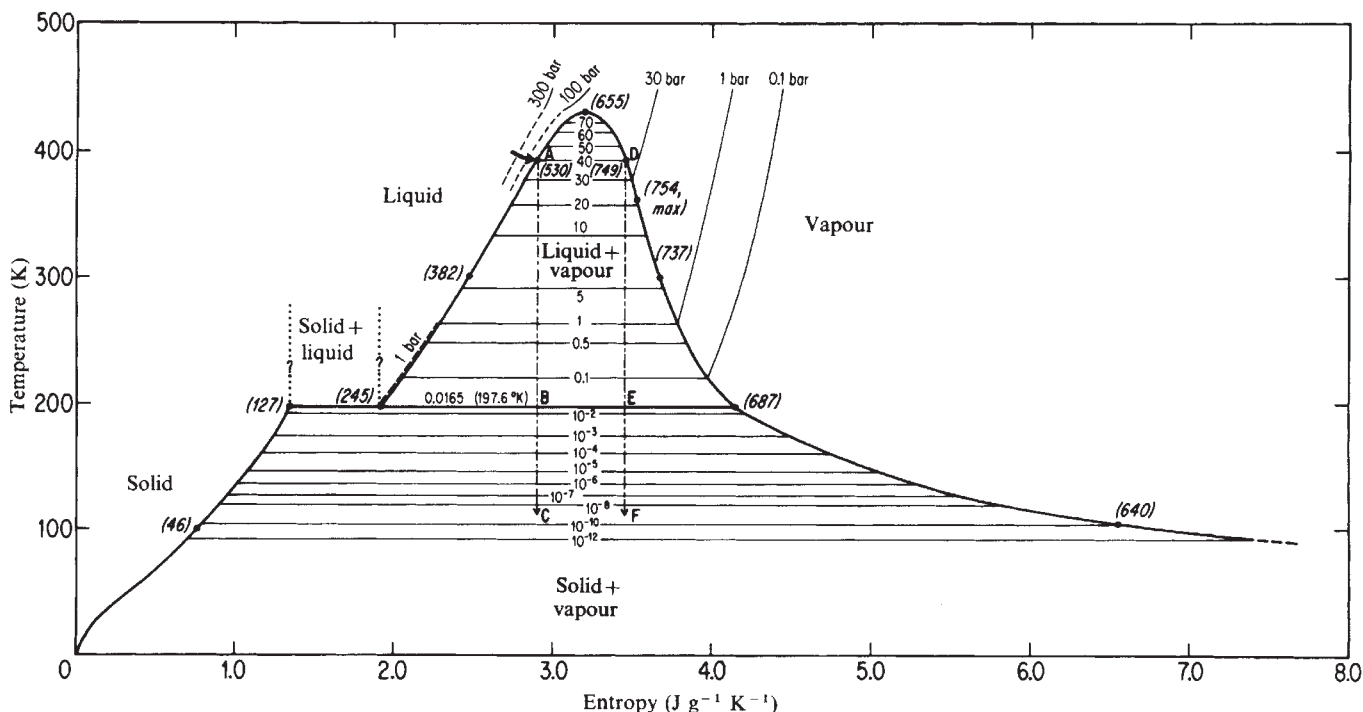


Fig. 1 Entropy-density relations in the SO₂ system. Heavy solid lines indicate the phase boundaries; heavy dashed or dotted lines are extrapolated beyond data sources; light lines represent isobars. Liquid-vapour equilibrium data from Braker and Mossman²⁶ adjusted to entropy equal 0.0 for the solid phase at 0 K by using the triple-point entropy and the enthalpy of fusion of Giauque and Stephenson²⁷. The solid sublimation curve was calculated from the heat capacities of Giauque and Stephenson by numerical integration. The vapour curve on the righthand side was calculated from heats of sublimation provided by D. D. Wagman (personal communication). The 1 bar and 30 bar isobars and all isobars in the liquid+vapour region are from vapour pressures listed by Braker and Mossman; the 0.1, 100, and 300 bar isobars are from data of Canjai and Manning²⁸. Isobars in the solid+vapour region are interpolated from vapour-pressure data provided by Wagman. Heavy arrow is pressure-temperature path of the sulphur liquidus, which intersects the SO₂ liquid-liquid+vapour phase boundary at point A. Isentropes ABC and DEF, shown with dot-dash lines, are discussed in text. Specific enthalpies are shown in parentheses.

Table 2 Mass fractions of vapour and velocities of SO₂ fluidised systems expanding isentropically from an initial state at 393 K and 40 bar

Pressure (bars)	Low entropy case (expansion from A in Fig. 1)		High entropy case (expansion from D in Fig. 1)	
	<i>x</i>	<i>u</i> (m s ⁻¹)	<i>x</i>	<i>u</i> (m s ⁻¹)
30.1	0.11	—	0.95	124
14.4	0.25	93	0.89	246
8.0	0.32	149	0.86	320
1.17	0.40	260	0.79	461
0.107	0.44	370	0.73	571
0.020	0.44	421	0.70	625
0.0165	0.55*	433*	0.75*	637*
1.9 × 10 ⁻³	0.52	488	0.70	689
9 × 10 ⁻⁵	0.48	550	0.64	752
7 × 10 ⁻⁷	0.44	610	0.58	815
8 × 10 ⁻⁹	0.41	680	0.52	870
4 × 10 ⁻¹²	0.35	737	0.40	965
0.00	0.00	1030	0.00	1224

*Calculated at the triple point when the liquid phase has just disappeared.

the range 10⁻⁷–10⁻¹² bar at the ground surface (that is, that the isobars of the atmosphere are not displaced large distances upward over the discharging vent) then, from the temperature–entropy diagram (Fig. 1), it can be concluded that the triple point is reached at depth before the fluidised system emerges from the surface. On the other hand, if the surface isobars are greatly displaced by the flow (the eruption plume ‘punches through’ the Io atmosphere), the triple point might be reached above the ground surface. At the triple point, the liquid droplets crystallise as the system expands isothermally and isobarically with an increase in vapour content to 55%. Further expansion is accompanied by condensation of SO₂ ‘snow’ from the vapour phase; at the time of exit to surface pressure, the vapour content of the system has decreased to 45–40% (depending on the surface pressure assumed) and, for the case considered, the velocity at the vent is 600 to 700 m s⁻¹. As the plume expands above the surface, SO₂ snow continues to form and the column continues to accelerate; if the plume were to break through the Io atmosphere and expand to approximately zero pressure and 0 K, the enthalpy converted to kinetic and potential energy would be equivalent to a velocity of 1.03 km s⁻¹, if the energy released were represented entirely by the kinetic energy term.

A different process occurs if the SO₂ system has an entropy higher than the critical point entropy on initiation of the eruption. Such a higher entropy could be attained either by (1) heating the SO₂ by incorporation of hot (sulphur) fragments or lapilli; or (2) segregation in the reservoir of the higher entropy vapour from the liquid SO₂, for example, across the 40 bar isobar in the temperature–entropy diagram; or by (3) intrusion of the heat source to shallow depth where the pressures are <40 bar. For any of these cases, the two-phase field is entered at the boundary with the vapour field rather than at the boundary with the liquid field, and isentropic expansion follows a path such as DEF shown in Fig. 1. The initial ascent and expansion of the system are accompanied by condensation of SO₂ liquid from the vapour; at the triple-point the condensed liquid freezes and further ascent is accompanied by condensation of solid from the vapour.

As a specific example of flow at an entropy higher than the critical point entropy, consider the same reservoir as discussed previously at 393 K, 40 bar, but with the vapour phase continuously segregated from the lower-entropy liquid (corresponding to the vapour side of the 40 bar isobar in Fig. 1). The entropy of the vapour is 3.46 J g⁻¹ K⁻¹ (point D) and its initial specific enthalpy is 749 J g⁻¹. As the vapour accelerates upwards, liquid is continuously condensed until triple point conditions are reached (point E). At this point, the SO₂ system consists of 70% vapour and is moving at 625 m s⁻¹ (again neglecting changes in potential energy). At the triple point the liquid freezes, the vapour content increases to 75%, and the system expands isobarically. Further ascent of the system is accompanied by condensation of SO₂ ‘snow’ from the vapour phase. At the time

of exit to surface pressure, the vapour content of the system has decreased to 55–50% and the exit velocity is in the range 850–950 m s⁻¹ (for surface pressures of 10⁻⁷–10⁻¹² bar). The theoretical maximum velocity obtainable (by expansion to zero pressure) is 1,224 m s⁻¹.

If acceleration of the fluidised system during expansion above the surface of Io is neglected, the maximum height above the surface reached by a parcel of the system leaving a vent at some exit velocity, *u*, will depend on the direction of its trajectory relative to the local vertical, which in turn is determined by the geometry of the vent itself. If we assume that the trajectory is purely ballistic, that most of the gas and entrained solids are ejected directly toward the local vertical, and that we can neglect the gravitational perturbations due to Jupiter, a given exit velocity, *u*, can be related to a maximum height, *h*, above the surface reached by the ejected material by

$$h = 2GM(V^2 - u^2)^{-1} - r_0 \quad (4)$$

where *V* is the two-body velocity of escape, *r*₀ the radius of Io, *M* the mass of Io, and *G* the gravitational constant. Taking 8.91 × 10²² g and 1,820 km for the mass and radius of Io and ignoring perturbations due to Jupiter, the velocity of escape from the surface of Io is 2.55 km s⁻¹. Assuming the plume expands to pressures of 10⁻⁷–10⁻¹² bar, the maximum heights reached by the decompression of pure SO₂ from the starting conditions at 393 K and 40 bar are 130–170 km for the low entropy case and 230–310 km for the high entropy case.

When computing actual escape trajectories, we cannot ignore the effects of Jupiter. For example, particles ejected vertically from the surface of Io directly towards or away from Jupiter with a velocity of 2.28 km s⁻¹ would reach the radius of the co-linear lagrangian points (*L*₁ and *L*₂) ~8,700 km above the surface and thus escape into circumjovian space. A more comprehensive discussion of this three-body problem as applied to Io is given by Smyth and McElroy¹⁷. When treating the near space within 300 km of Io's surface, however, the magnitude of Jupiter's perturbations remains <0.003 and the effects on equation (4) are negligible.

A slightly more stringent requirement on the vent exit velocities than the height of plumes is given by the maximum distance to which material has been deposited on the surface of Io by the plumes. Each deposit records the maximum range over the life of the plume. In the case of Plume 1, the most distant limit of the recognisable deposit is 700 km (22°) from the eruptive centre. The minimum velocity at which material can be ejected to this range on a simple ballistic trajectory is given by

$$u = \left(\frac{2r_0g_0}{\cot(\phi/2) + 1} \right)^{1/2} \quad (5)$$

where *g*₀ is the gravitational acceleration at the surface (179 cm s⁻²); and *φ* the range in planetocentric angular distance from the vent. For a range *φ* of 22° for the limit of the deposit of Plume 1, *u* is 1.03 km s⁻¹.

Significant departures from purely ballistic trajectories of material in the plumes are caused by expansion of the gas in the plumes and probably also by shocks. Expansion in the plumes provides a moderate increment of velocity after exit from the vent, whereas shocks influence the flow in the gas and details of the shapes of the plumes and trajectories of initially entrained particles¹⁸. We can conclude, however, that SO₂ gas and condensed particles can be accelerated to velocities required to explain the highest of the observed plumes, starting from temperatures close to the sulphur liquidus, so long as the plumes are nearly free of entrained initially cold material. A temperature slightly higher than the melting point of monoclinic sulphur at 40 bar (393 K) may be required to explain the most distant deposits of Plume 1.

Addition of cold solid material to the fluidised system expanding up the vent, by spalling of the walls of the vent, for instance, will decrease the velocity of the system. If all this material is entrained, the kinetic energy of the fluidised system

must be distributed through a larger mass. If the mass of the system is doubled, for example, the velocity will decrease by a factor of $\sqrt{2}$. On the other hand, if liquid sulphur is entrained, the decrease in velocity is very much less than for cold wall rock. This is because the enthalpy of the sulphur droplets becomes converted to kinetic energy as the fluidised system expands and cools. Entrained sulphur is probably reduced to particles comparable in size to volcanic ash produced in violent gaseous eruptions in terrestrial volcanoes of the order of 1 mm or less. Drops of this size will very quickly come to approximate thermal equilibrium with the gas, releasing both the heat of fusion, $\sim 38 \text{ J g}^{-1}$, as the drops freeze, and about $0.75 \text{ J g}^{-1} \text{ K}^{-1}$, as the frozen sulphur ash cools to temperatures of the order of 100 K. The total specific enthalpy released by cooling liquid sulphur to 100 K is about 260 J, which is about half of the specific enthalpy released by adiabatic expansion of the entraining SO_2 gas. Hence, fairly large mass fractions of initially liquid sulphur can be entrained in the eruptive column without seriously decreasing the vent exit velocity of the plume.

Observations made by Voyager I are consistent with the interpretation that elemental sulphur is a common constituent of the surface of Io. Abundant flows of low relief, ranging in colour from red to yellow, radiate from many caldera-like features^{19,20}. These flows have lengths of up to several hundred kilometres, and many apparently have very low gradients. They were formed, therefore, by fluids of viscosity comparable to or less than the viscosity of lunar basaltic lavas, $\sim 10^2\text{--}10^4 \text{ P}^{21}$. Molten sulphur at all temperatures is a fluid of appropriately low viscosity²⁰. Moreover, because of the low melting point of sulphur, the rate of heat loss from sulphur flows would be two orders of magnitude lower than for silicate lava flows, which further facilitates the development of comparatively great flow length.

Many calderas are occupied by material of very low albedo resembling lava lakes^{1,19,22}. In one case, a black horseshoe-shaped 'lava lake' $\sim 200 \text{ km}$ across (Plate 1, p. 782) has a model-derived temperature about 150 K above that of the surrounding surface²³. Thermal observations suggest that this feature is an active lake of molten sulphur with a partial, very thin, chilled crust. Of special interest is that although this 'lake' lies within the fallout area of Plume 2, no fallout deposit is recognisable on its surface. The albedo of the 'lake' is appropriate for molten sulphur at temperatures in the range of 500 K and above²⁰. The black colour of the liquid may be partly preserved in chilled crusts by quenching²⁰. We interpret all the black features resembling lava lakes distributed across the surface of Io as active or recently active lakes of molten sulphur.

Except at the 'lava lakes' and possibly other active lava surfaces, the surface temperature of Io is well below the freezing point of SO_2 (198 K at 1 bar). The widely distributed white patches, illustrated elsewhere¹, could well be optically thick deposits of SO_2 frost, although a very white form of elemental sulphur has also been suggested²⁰. SO_2 may also be adsorbed on sulphur (or other constituents) on the yellow parts of Io's surface. Any plume-supplied SO_2 , leading to a surface pressure somewhat in excess of the mean daytime (130 K (ref. 23)) vapour pressure of solid $\text{SO}_2 \sim 1.4 \times 10^{-7} \text{ bar}$ (Fig. 3), would result in precipitation of SO_2 frost and the build up of frost deposits that are stable through the day. Frost would tend to accumulate preferentially in areas that remain coldest during the diurnal temperature cycle. At a given latitude the areas that remain coldest are those with the highest albedo—the white patches themselves. This positive feedback mechanism may explain the patchy distribution of the frost and the fact that lava flows recently extruded onto the surface apparently remain frost-free (at least during the day).

Models of the crustal structure of Io, which are necessary for a theoretical understanding of the dynamics of the plumes, can be derived from an estimate of mean density of the satellite, estimates of the rate of heat production by tidal dissipation, and the interferences about the surface composition. The mean density of Io, 3.53 g cm^{-3} (ref. 1), suggests that the satellite is

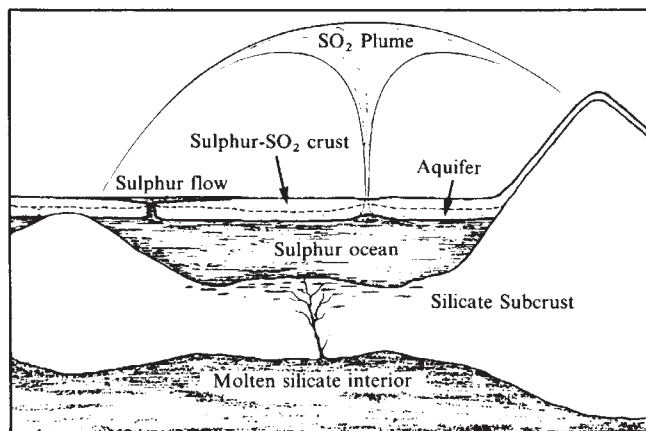


Fig. 2 Proposed crustal structure for Io. Heights and thicknesses are not drawn to scale. The uppermost layer, which also covers all solid silicate topography, is composed of a mixture of solid SO_2 and sulphur. The subjacent layer is a porous solid sulphur aquifer through which liquid SO_2 flows freely. Below this is a molten sulphur 'ocean' which rests on a solid silicate subcrust overlying a uniformly melted silicate interior. Where the upper crust is less buoyant, molten sulphur will flow over the surface. A plume is created when liquid SO_2 pours into an open vent left by a receding molten sulphur intrusion. Intruded silicate sills build up at the bottom of the sulphur ocean.

composed predominantly of ferromagnesian silicates and that it has a substantial iron or iron sulphide core. The model for Io proposed by Peale *et al.*⁴ before the Voyager discovery of volcanism contained a uniformly melted interior surrounded by a 20 km thick silicate crust with an implied surface heat flux of $\sim 500 \text{ erg cm}^{-2} \text{ s}^{-1}$. More detailed models of the crust depend critically on the assumed ratio of free sulphur to silicates in the crust. As discussed by Carr¹⁹, sulphur dissolved in silicate magmas exsolves as the magmas rise to the surface and, in terrestrial volcanoes, condenses on the surface or in near surface voids. This condensed sulphur is then remobilised as a melt if it is buried and reheated, a process which has occurred on Earth where sulphur lava flows have been noted. Buildup of the Io crust by repeated extrusion of sulphur-saturated silicate lavas would result in continued enrichment of sulphur in the upper part of the crust by remobilisation and upward migration of the free sulphur both as a gas and as a melt.

Carr¹⁹ suggests that both sulphur and silicate lava flows are present around many caldera-like eruptive centres on Io. If this is so, the solid crust of Io consists predominately of silicates, with a subordinate amount of sulphur concentrated in the upper part. However, injection of a column of silicate magma into a solid sulphur upper crust would quickly lead to melting of a volume of sulphur larger than the volume of the silicate column; the higher density silicate magma could not then rise buoyantly through the fluid sulphur unless it were expanded by vesiculation to a density less than that of molten sulphur ($\sim 1.8 \text{ g cm}^{-3}$).

We prefer a model in which the upper crust consists largely of elemental sulphur and SO_2 and overlies a subjacent layer of molten sulphur possibly several kilometres thick (Fig. 2). In the upper crust, sulphur is present both as lava flows and as interstratified pyroclastic deposits. The rate at which temperature increases with depth in the upper crust depends both on the local coefficient of thermal conductivity of the sulphur and the frozen SO_2 and the value of the net outward heat flux. Of the two, the latter is by far the more difficult to estimate. In our model, we use a conservative value for the heat flux generated by tidally dissipated energy in the silicate lower crust, $100 \text{ erg cm}^{-2} \text{ s}^{-1}$. Of this total, using resurfacing rates estimated by Johnson *et al.*³, $25 \text{ erg cm}^{-2} \text{ s}^{-1}$ escapes through volcanism, leaving $75 \text{ erg cm}^{-2} \text{ s}^{-1}$ to be conducted upward through the crust. The lower crust (a few km to $\sim 20 \text{ km}$ depth) is composed mainly of a complex of silicate sills that have been intruded successively at the base of the molten sulphur layer. These intrusives are more

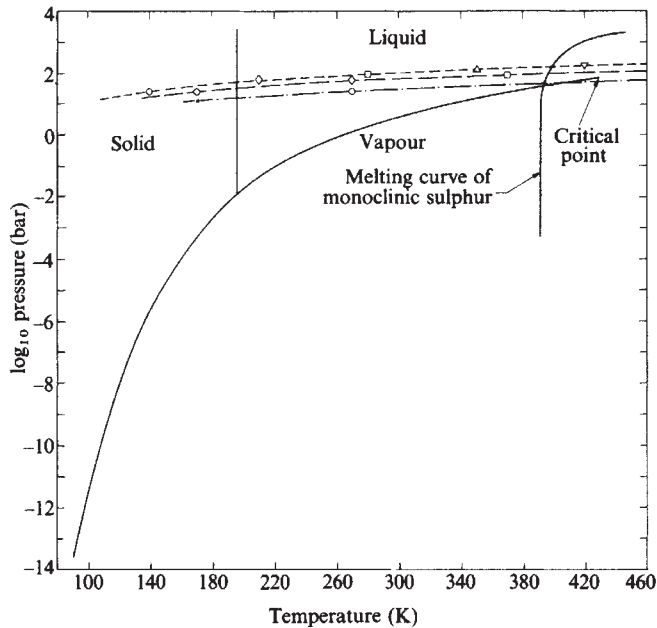


Fig. 3 Pressure-temperature phase diagram for SO_2 showing the relationship of three assumed geotherms on Io to the boundaries of the phase fields. Boundaries of phase fields are derived from data given by Braker and Mossman²⁶, Giaouque and Stephenson²⁷ and Wagman. The geotherm 200 K km^{-1} is believed to be close to the actual pressure-temperature profile in the upper (sulphur) crust of Io. Depths plotted on the geotherms are calculated for densities of 1.45 g cm^{-3} up to 1 km and 1.89 g cm^{-3} below 1 km (corresponding to a porous sulphur- SO_2 permafrost zone to 1 km and a zone of porous sulphur saturated with liquid SO_2 below 1 km). \odot , 0.5 km; \square , 1 km; \diamond , 2 km; \square , 3 km; \triangle , 4 km; ∇ , 5 km; --- 70 K km^{-1} ; - - - 100 K km^{-1} ; — 200 K km^{-1} .

and more thermally metamorphosed towards the base of the lower crust where, again, complete remelting defines the base.

Recycling of the sulphur upper layer is independent of the cycling of the silicate lower layer. Temperatures of sulphur melts erupting at the surface will tend to be close to the melting point of sulphur.

The limiting thickness to which the sulphur upper layer can evolve is that at which the pore pressure at the base of the sulphur layer is just equal to the mean sulphur vapour pressure of the silicate magmas intruded at its base. Studies by Haughton *et al.*²⁴ suggest that silicate magmas with sulphur vapour pressure high enough for the sulphur upper layer to evolve to several kilometres thickness (S_2 vapour pressure ~ 100 bar) must have very low contents of FeO.

SO_2 frost precipitated on the surface of Io tends to be buried under pyroclastic fallout from the eruptive plume systems, and, if sufficiently insulated by pyroclastic deposits, it can also be buried beneath sulphur flows. Thus, as volcanic material accumulates on the surface, some of the frost deposits are trapped and carried down in the volcanic cycling of the crust. As temperatures rise with increasing depth of burial, the trapped SO_2 probably migrates to some extent and recrystallises in irregularly distributed bodies of ground ice.

Assuming the nominal heat flux given above and a temperature-dependent, thermal conductivity of $3\text{--}5 \times 10^{-3} \text{ W cm}^{-1} \text{ K}^{-1}$ for the permafrost zone, the 198 K isotherm (freezing level of SO_2) will lie at depths between 500 and 1,000 m; depths to this isotherm will be greatest at the poles and least at the equator. Below this isotherm the trapped SO_2 is liquid and forms an interstitial ground fluid that, if sufficiently abundant, tends to saturate all permeable strata. The SO_2 ground fluid freezes out wherever it reaches the 198 K isotherm and tends to seal the base of the overlying SO_2 permafrost zone to produce an effective 'aquaclude'.

The base of the SO_2 liquid zone will be defined either by contact with molten sulphur or by intercept of the local geotherm of Io with the SO_2 vapour field (Fig. 3). For thermal

gradients of the order of 200 K km^{-1} or somewhat steeper consistent with the heat flow and thermal conductivity we have adopted, the SO_2 liquid zone will be $\sim 500\text{--}1,000$ m thick, and it will be underlain by a thin SO_2 vapour zone. If the total abundance of SO_2 in the crust is high enough, the SO_2 liquid zone may be saturated or nearly saturated throughout.

If the SO_2 liquid zone is saturated, it will be an artesian system, driven by the pressure of liquid sulphur or SO_2 vapour at the base of the zone. In this case, liquid SO_2 will flow towards any locus where fluid escapes and where there is a corresponding pressure drop⁹. If many such loci of fluid escape are distributed over the surface of Io, the regional flow of SO_2 ground fluid will tend to be up the pressure gradient, towards the shallowest parts of the 198 K isotherm. Hence, the regional flow will tend to be from the polar regions to the equator, possibly from the regions of white patches to frost-free regions and, most importantly, from regions of average thermal gradient towards active plume vents.

All but one of the known eruptive plumes on Io occur at latitudes $\leq 30^\circ$ (ref. 2). Assuming that the plumes are driven by SO_2 , this distribution suggests that the SO_2 liquid zone is, in fact, nearly saturated and that regional artesian flow occurs from the polar regions to the equatorial regions. If only a small fraction of the SO_2 liquid zone were saturated, most or all of this zone at low latitudes might be above the regional SO_2 liquid table and insufficient SO_2 would be available to form the eruptive plumes.

The melting point of sulphur is probably reached at depths of the order of 1,500 m below the surface. In places where convective flow of the SO_2 ground fluid can occur, the thermal gradients will be less steep and the top of the molten sulphur layer may be deeper. Where the sulphur is thick enough, the molten sulphur constitutes a sulphur 'ocean' or 'thiosphere'²⁰ extending downwards to the lower silicate crust, possibly several kilometres below. The solubility of SO_2 in liquid sulphur is ~ 0.02 (mass fraction): thus SO_2 may also be transported over global distances by currents within the sulphur ocean.

The upper crust of solid sulphur and solid and fluid SO_2 rests buoyantly on the sulphur ocean. The upper crust is buoyant because of pore space in the SO_2 permafrost zone, probably on the order of several tens of per cent, and the admixture of low density solid SO_2 ($\sim 1.6 \text{ g cm}^{-3}$), in the solid sulphur ($\sim 2.0 \text{ g cm}^{-3}$), and because of the low density of the liquid SO_2 ($\sim 1.5 \text{ g cm}^{-3}$) that fills the pore space in the SO_2 liquid zone. As the SO_2 liquid zone is probably sealed at the base of the permafrost, pore pressure in the liquid SO_2 can approach the lithostatic pressure. Hence, if the SO_2 liquid zone is saturated, collapse of pores is retarded until the SO_2 vapour zone is reached. Wherever the base of the sulphur upper crust exceeds the density of liquid sulphur, (1.8 g cm^{-3}) as result of loss of pore space, it will tend to founder into the sulphur ocean.

The overall buoyant freeboard of the sulphur crust is maintained by delamination or foundering of the base but probably remains small. Wherever the freeboard is negative, liquid sulphur can rise to the surface to form a sulphur volcano. Rapid rise of sulphur along a new fissure will result in chilling of the sulphur against the fissure walls. A layer of frozen sulphur along the chilled margins probably seals the fissure against inflow of liquid SO_2 . In most cases, cessation of sulphur magma flow at an immature vent probably results in complete freezing of sulphur in the vent and no loss of SO_2 fluid at the surface.

At more mature conduits, where prolonged flow of sulphur has heated the vent walls (perhaps those vents that feed lava lakes) there may be a different denouement of a sulphur volcano. When local foundering at the base of the sulphur crust occurs, the crust will bob up buoyantly, and the level at the top of the liquid sulphur column will abruptly subside relative to the surface. Because the top of the liquid SO_2 zone surrounding a mature vent may be near the surface, withdrawal of the sulphur column allows the SO_2 to flow into the vent, initiating a 'phreatic' eruption. By this means a plume is born. The suggested mechanism for initiating the plumes is analogous to the mechanism of rare phreatic eruptions at Kilauea, Hawaii, which

occur after major withdrawals of lava in the caldera that allow groundwater to flow into the vent²⁵. Where the flow of SO₂ ground fluid is high enough, the top of the liquid sulphur column will be eroded by the expanding fluidised SO₂ system, and the base of the expanding system may descend deep into the sulphur crust. The plume may be extinguished when the liquid SO₂

available to drain into the vent is exhausted or, more likely, when the rate of upwelling of liquid sulphur in the vent exceeds the loss to the fluidised column at the top. This could occur after the SO₂ liquid table around the vent has been deeply drawn down by prolonged discharge. The rising liquid sulphur column will then shut off the SO₂ flow.

Received 19 July; accepted 9 August 1979.

1. Smith, B. A. *et al. Science* **204**, 951-972 (1979).
2. Strom, R. G., Terrile, R. J., Masursky, H. & Hansen, C. *Nature* **280**, 733-736 (1979).
3. Johnson, T. V. *et al. Nature* **280**, 746-750 (1979).
4. Peale, S. J. *et al. Science* **203**, 892-894 (1979).
5. Fanale, F. P., Hamilton Brown, R. & Cruikshank, D. P. *Nature* **280**, 761-763 (1979).
6. Smythe, W. D. *et al. Nature* **280**, 766 (1979).
7. Kumar, S. *Nature* **280**, 758-760 (1979).
8. Pearl, J. *et al. Nature* **280**, 755-758 (1979).
9. McCauley, J., Smith, B. A. & Soderblom, L. A. *Nature* **280**, 736-738 (1979).
10. Broadfoot, A. L. *et al. Science* **204**, 972 (1979).
11. Krimigis, S. M. *et al. Science* **204**, 998-1002 (1979).
12. Wamsteker, W. *et al. Icarus* **23**, 417 (1974).
13. Nash, D. B. & Fanale, F. P. *Icarus* **81**, 40 (1977).
14. Nelson, R. & Hapke, B. *Icarus* **36**, 304 (1978).

15. Fanale, F. P. *et al. Science* **186**, 922 (1974).
16. Self, S. *et al. Nature* **277**, 440 (1979).
17. Smyth, W. H. & McElroy, M. B. *Planet Space Sci.* **25**, 415 (1977).
18. Cook, II, A. F. *et al. Nature* **280**, 743-746 (1979).
19. Carr, M. H. *et al. Nature* **280**, 729-733 (1979).
20. Sagan, C. *Nature* **280**, 750-753 (1979).
21. Cukierman, N., Tutts, P. N., & Uhmman, D. R. *Geochim. cosmochim. Acta Supl* **3**, 2619 (1972).
22. Masursky, H. *et al. Nature* **280**, 725-729 (1979).
23. Hanel, R. *et al. Science* **204**, 972-976 (1979).
24. Haughton, D. R. *et al. Econ. Geol.* **69**, 451 (1974).
25. Finch, R. H. *Pacif. Sci.* **1**, 237 (1947).
26. Braker, W. & Mossman, A. L. *Matheson Gas Data Book*, 5th edn, 513 (C. Rutherford, New Jersey, 1971).
27. Giauque, W. F. & Stephenson, C. C., *J. Am. chem. Soc.* **60**, 1389 (1938).
28. Canjai, L. N. & Manning, F. S. *Thermodynamic Properties and Reduced Correlations for Gases*, 169 (Gulf Publishing Co., Houston, 1969).

Dynamics of volcanic plumes on Io

A. F. Cook*, E. M. Shoemaker† & B. A. Smith‡

* Center for Astrophysics, Harvard College Observatory and Smithsonian Astrophysical Observatory, Cambridge, Massachusetts 02138
 † US Geological Survey, Flagstaff, Arizona 86001
 ‡ Department of Planetary Sciences, University of Arizona, Tucson, Arizona 85721

Ballistic and aerodynamic models are proposed to explain the volcanic plumes on Io, with particular reference to Plumes 1 and 3 which seem to have the same origin.

VARIOUS clues suggest that aerodynamics play a role in the volcanic plumes on Io which were revealed by the cameras on Voyager 1¹. These are: (1) the formation of a more or less circular ring or double ring about the vent, the region of the ring being a bland one obviously covered over by frost or crystals or entrained particles from the plume; (2) the filamentary structure of the upper regions of Plume 1 (*Plate 6b*, p. 788) as shown in a picture taken near the limb; and (3) abrupt bends in each of the individual dark filaments along trajectories in Fig. 1 which shows Plume 3 taken as it was becoming visibly active on the disk.

The ballistic model

We assume that the rate of flow of gas is sufficiently small from our volcanic vent so that gas and solid particles become completely decoupled over a distance small compared with the maximum height reached by the particles and remain decoupled. In that case a convenient model starts all particles through a circular orifice with a common velocity diverging from a common point below the centre so that the velocity vectors uniformly fill a cone with a vertical axis and opening out toward the zenith. We shall show that this model does not fit the observed structure of the plumes.

Let r denote radial distance (Fig. 2), z the height above the surface, t the time, z_0 the depth of the vertex of the launch cone, v_0 the effective launch velocity at that depth, and t_0 the effective epoch of passage through the vertex. We neglect the curvature of Io's surface and the variation of its acceleration of gravity g , with height. The equations of motion and initial conditions are:

$$\left. \begin{aligned} d^2z/dt^2 &= -g, & d^2r/dt^2 &= 0, & dz/dt|_{t=t_0} &= v_0 \cos i, \\ dr/dt|_{t=t_0} &= v_0 \sin i, & z|_{t=t_0} &= -z_0 & \text{and } r|_{t=t_0} &= 0 \end{aligned} \right\} (1)$$

where i denotes the launch angle measured from the zenith. Elimination of the time and solution for the two values of i which will dispatch particles through a given position (r, z) yields:

$$\cot i = \frac{v_0^2}{gr} \left\{ 1 \pm \left[1 - \left(\frac{gr}{v_0^2} \right)^2 - 2 \frac{g(z_0 + z)}{v_0^2} \right]^{1/2} \right\} \quad (2)$$

The two solutions coalesce at an upper envelope at which the square root vanishes

$$z_M = -z_0 + \frac{v_0^2}{2g} - \frac{gr^2}{2v_0^2}, \quad \cot i_M = \frac{v_0^2}{gr} \quad (3)$$

where the subscript M denotes the upper envelope. The outer edge of the launch cone is at i_0 and this sets a limit on the envelope at

$$r_1 \equiv \frac{v_0^2}{g} \tan i_0, \quad z_1 = \frac{v_0^2}{2g} (1 - \tan^2 i_0) - z_0 \quad (4)$$

where the subscript 1 denotes this ring. The curve for $i = i_0$ will act as a lower bound for one of the two solutions for $\cot i$ (lower sign) out to (r_1, z_1) :

$$z_m = -z_0 + r \cot i_0 - \frac{gr^2}{2v_0^2} \operatorname{cosec}^2 i_0 \quad (5)$$

where the subscript m denotes this lower bound for populated double solutions for i . This lower bound should provide an internal surface within the plume. Beyond and below (r_1, z_1) the surface equation (5) becomes an outer bound on the plume terminating at $(r_m, 0)$:

$$r_m = \frac{v_0^2}{g} \sin i_0 \left[\cos i_0 + \left(\cos^2 i_0 - \frac{2gz_0}{v_0^2} \right)^{1/2} \right] \quad (6)$$

Should z_1 lie below Io's surface, the surface, equation (3), would terminate at $(r_M, 0)$:

$$r_M = \frac{v_0^2}{g} \left(1 - \frac{2gz_0}{v_0^2} \right)^{1/2} \quad (7)$$

The surface, equation (5), also has an inner intersection with Io's surface at the radius r_p , of the orifice:

$$r_p = \frac{v_0^2}{g} \sin i_0 \left[\cos i_0 - \left(\cos^2 i_0 - \frac{2gz_0}{v_0^2} \right)^{1/2} \right] \quad (8)$$